



# Calculation of the three-dimensional sound pressure field around bodies with macro porosities

Bin Wang, Denis Duhamel

## ► To cite this version:

Bin Wang, Denis Duhamel. Calculation of the three-dimensional sound pressure field around bodies with macro porosities. The 21st International Congress on Sound and Vibration, Jul 2014, Beijing, China. hal-01118273

**HAL Id: hal-01118273**

**<https://hal.science/hal-01118273>**

Submitted on 2 Mar 2015

**HAL** is a multi-disciplinary open access archive for the deposit and dissemination of scientific research documents, whether they are published or not. The documents may come from teaching and research institutions in France or abroad, or from public or private research centers.

L'archive ouverte pluridisciplinaire **HAL**, est destinée au dépôt et à la diffusion de documents scientifiques de niveau recherche, publiés ou non, émanant des établissements d'enseignement et de recherche français ou étrangers, des laboratoires publics ou privés.



## CALCULATION OF THE THREE-DIMENSIONAL SOUND PRESSURE FIELD AROUND BODIES WITH MACRO POROSITIES

Bin Wang, Denis Duhamel

*Université Paris-Est, Laboratoire Navier, ENPC-IFSTTAR-CNRS, UMR 8205, Ecole des Ponts ParisTech, 6-8 avenue Blaise Pascal, 77455 Marne-la-Vallée, France,  
e-mail: bin.wang@enpc.fr*

This paper proposes a multi-domain boundary element method to compute the sound field around bodies with macro porosities. It saves computational cost and is especially suitable for complex structures. It is based on the boundary element method, and divides the computation into an exterior subdomain and several interior subdomains. The subdomains are connected by transfer matrices. This method is applied to study some simple examples for which analytical or BEM results are available. Good agreements between these known solutions and the results of multi-domain BEM can check the accuracy. Then a complicated network with flange is calculated with multi-domain BEM to show the influence of network on sound pressure field.

### 1. Introduction

Systems with large porosities can be seen in the analysis of porous noise barriers, horn effect of road/tire and so on. It is essential to calculate the sound pressure field around them.

In such systems, the waveguides to be analyzed have small cross sections. However, it is neither as small as the arbitrary microscopic holes in many porous materials nor as big or complicated as the pipes in the mufflers, so it is not suitable to use the same methods to calculate the sound pressure field of the flanged waveguide. But the methods for mufflers could give some inspirations. Mufflers have complicated internal structures. There are several methods for the analysis of mufflers summarized in [1]. The multi-domain boundary element method (BEM) and BEM with the transfer matrix could be used for the calculation of the flanged waveguide, but some changes should be made.

A brief introduction of the applications of multi-domain BEM can be seen in [2]. It was first used to analyze the potential problem and elasticity [3]. Then it was introduced to solve acoustic problems. An important application of multi-domain BEM to acoustics is the coupled interior/exterior problems [4]. The multi-domain BEM is also used to deal with problems with several acoustic media [5]. Another wide application is the problem about thin bodies [6] before using the hypersingular integral equation. Dividing the whole acoustic domain into several subdomains is the main idea of the multi-domain BEM. Substructuring can reduce the matrix size and the total computational time for large structures, but the adjacent subdomains should have the same interface mesh to match the boundary conditions.

Transfer matrix techniques have been applied to the analysis of series of connected pipes with many changes of sectional area in [7]. In [8] a different form of transfer matrix is used, together

with the matrices derived for the two-dimensional junctions by finite element method, to describe a complete network. In [9] the transfer matrix is used to combine the impedance matrix of each substructure of a silencer. The transfer matrix can easily connect two substructures and describe the relation of pressure and particle velocity between them. But an assumption should be true to get the transfer matrix, which is the plane wave propagation in the connected part.

For the waveguide analyzed in this paper, BEM is available, but only for very simple case as BEM needs fine mesh around the resonant frequency of the waveguide to get converged solutions. However, since BEM is advantageous for analyzing problems with an exterior domain or a complex geometry, a substructuring technique based on BEM is proposed to reduce matrix size of the structure, and also a modified transfer matrix is used to connect the subdomains to reduce the nodes and elements and avoid the identical mesh at the interface.

First the structure to be analyzed and wave propagation are introduced. The computational method is described in the next section. Then comparisons are given to check the accuracy of the proposed method. Finally a complicated case is solved with the proposed method.

## 2. Problem specification

### 2.1 Wave propagation

The structure to be analyzed in this paper has arbitrary flange and a macro porosity. The waveguides constituting the porosity could have any connection pattern: arbitrary network, parallel pipes or a mixture of them. The pipes in this paper have small cross sections.

Fig.1a represents three dimensional network with arbitrary flange. Put a point source  $S$  near the flange. The acoustic wave at point  $R$  includes three parts (see Fig.1a): wave directly from the source, wave reflected from the flanged without network (see Fig.1b) and wave radiating from the network with flange (see Fig.1c). The wave from the source arrives at pipes ends and then propagates in the network. The straight parts of the network are very thin compared with the wave length to be analyzed. So there is only plane wave motion in the straight parts. The wave in the junction of the network has higher order modes, but it doesn't propagate in the straight parts. In Fig.1b, we use imaginary pipes ends instead of the real ends. The imaginary ends are inside the network but close to the real ones. The imaginary surfaces  $S_{imag}$  are perpendicular to pipes walls. Thus, at  $S_{imag}$  the wave is uniform, which can be useful in the method proposed in this paper. However, it is not uniform at the real ends, even if the real ends are perpendicular to the network walls, because the cross sections change suddenly.

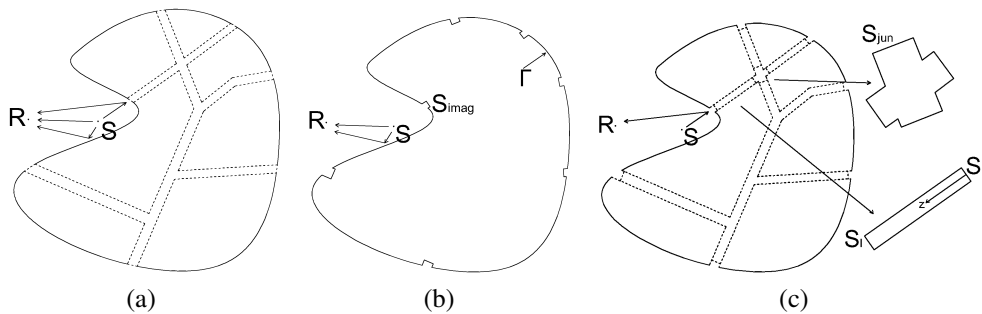


Figure 1: (a) Total pressure; (b) Pressure directly from source and reflected by flange; (c) Pressure radiating from network

### 2.2 Boundary condition

The boundary condition of flange and waveguide walls could be the pressure, the normal derivative of the pressure, the impedance, the surface velocity, or a mixture of them. There should be a small

transition zone between different boundary conditions.

### 3. Computational method

The calculation of the total acoustic pressure  $p_{tot}$  at a point  $R$  in the exterior domain in Fig.1a is the task of this paper.

#### 3.1 The total pressure

The waveguide to be analyzed consists of cylindrical or rectangular pipes with small cross sections. For very simple waveguides one can get the total pressure easily by running BEM once. However, around the resonant frequency of the waveguide it needs fine mesh to get converged results by BEM. So the computational costs are very high. For complicated networks, fine mesh leads to memory problem of computer. To avoid this problem, a multi-domain BEM combined with transfer matrix technique is proposed.

In boundary element methods, for a problem with a bounded domain, the integral equation to be solved is given by

$$c_e(\mathbf{x})p(\mathbf{x}) = \int_{\Omega} p(\mathbf{y}) \frac{\partial G}{\partial \mathbf{n}_y}(\mathbf{x}, \mathbf{y}) d\mathbf{y} - \int_{\Omega} \frac{\partial p}{\partial \mathbf{n}_y}(\mathbf{y}) G(\mathbf{x}, \mathbf{y}) d\mathbf{y} + p_{inc}(\mathbf{x}) \quad (1)$$

$\Omega$  is the surface of a bounded domain.  $p_{inc}(\mathbf{x})$  is the incident pressure from the source without the structure.  $G$  is the Green function.  $\mathbf{n}$  is the unit normal vector pointing into the domain. To get the total pressure  $p_{tot}$  in the exterior domain, let  $c_e(x) = 1$ ,  $p_{inc}(x) = 0$  and surface  $\Omega$  be  $\Gamma$ .  $\Gamma$  includes the flange and the imaginary network ends (see Fig.1b). Substitute pressure  $p(\mathbf{y})$  and its derivative  $\frac{\partial p}{\partial \mathbf{n}_y}$  on the surface  $\Gamma$  into Eq. (1) and solve it, one has  $p_{tot}$ . These values should be calculated first.

#### 3.2 Unknowns on surface $\Gamma$

Divide the problem in Fig.1a into an exterior subdomain of flange and several interior subdomains of junctions. Solve each subdomain by BEM to get BEM system matrices and excitation vector, and then connect the subdomains by transfer matrices. Finally solve the overall equation system, and one has  $p(\mathbf{y})$  and  $\frac{\partial p}{\partial \mathbf{n}_y}$  on surface  $\Gamma$ . The process is described in detail in the following.

##### 3.2.1 Subdomains

In Eq. (1), for a point  $\mathbf{x}$  on  $\Omega$ ,  $c_e(\mathbf{x})$  equals 1/2 if the surface  $\Omega$  is regular at this point. The discretization of Eq. (1) is obtained from a mesh of the surface of the domain. Then a linear system (2) can be obtained whose solution gives an approximation of the solution on the surface  $\Omega$ . More information can be found in [10].

$$\mathbf{A}\mathbf{P} + \mathbf{B}\mathbf{Q} = \mathbf{P}_{inc} \quad (2)$$

$\mathbf{P}$ ,  $\mathbf{Q}$  and  $\mathbf{P}_{inc}$  are vectors of pressure, derivative of pressure and incident pressure, respectively.  $\mathbf{A}$  and  $\mathbf{B}$  are BEM system matrices.

For the exterior subdomain in Fig.1b, divide the vectors in Eq. (2) into vectors of imaginary ends and vectors of flange. One has

$$\mathbf{A}_E \begin{bmatrix} \mathbf{P}_{ep} \\ \mathbf{P}_f \end{bmatrix} + \mathbf{B}_E \begin{bmatrix} \mathbf{Q}_{ep} \\ \mathbf{Q}_f \end{bmatrix} = \begin{bmatrix} \mathbf{P}_{inc}^{ep} \\ \mathbf{P}_{inc}^f \end{bmatrix} \quad (3)$$

The subscripts and superscripts  $ep$  and  $f$  mean the imaginary ends of straight pipes and the flange, respectively. Matrices  $\mathbf{A}_E$  and  $\mathbf{B}_E$  can be obtained by solving the problem in Fig.1b with BEM software. In the BEM software, using the rigid boundary condition on the surface  $\Gamma$ , one can get  $\mathbf{A}_E$ . Using the soft boundary condition, one can get  $\mathbf{B}_E$ . The incident pressure  $p_{inc}$  can be obtained in either of the two computations above.

For the network in Fig.1c we create imaginary surfaces for its junctions. These surfaces should be perpendicular to the network walls. One can see the interior subdomain of a junction in Fig.1c. The normal direction of surface  $S_{jun}$  points inward. Since for the junction subdomain there is no source, the incident pressure equals zero. The equations system for the junction is

$$\mathbf{A}_I \begin{bmatrix} \mathbf{P}_{ej} \\ \mathbf{P}_w \end{bmatrix} + \mathbf{B}_I \begin{bmatrix} \mathbf{Q}_{ej} \\ \mathbf{Q}_w \end{bmatrix} = \begin{bmatrix} \mathbf{0} \\ \mathbf{0} \end{bmatrix} \quad (4)$$

The subscripts and superscripts  $ej$  and  $w$  mean the imaginary ends and the walls of junction. Matrices  $\mathbf{A}_I$  and  $\mathbf{B}_I$  can be obtained by running the BEM software in the same way as before.

### 3.2.2 Transfer matrix

The straight pipe between the flange and the junction or two junctions in Fig.1c, whose central axis is labelled as  $z$ , is thin compared to the wave length to be analyzed. There is only plane wave. Pressure  $p$  and its derivative  $q$  are constant on a plane perpendicular to  $z$ . The wave equation is

$$\frac{\partial^2 p}{\partial z^2} = \frac{1}{c^2} \frac{\partial^2 p}{\partial t^2} \quad (5)$$

$c$  is the sound speed. Suppose that the solution of Eq. (5) is

$$p(z) = a \cos kz + b \sin kz \quad (6)$$

$k$  is the wave number. The convention  $e^{-i\omega t}$  is adopted, where  $i^2 = -1$ ,  $\rho$  is the density of air and  $\omega$  is the angular frequency. The velocity is given as

$$v(z) = \frac{1}{i\rho\omega} \frac{\partial p}{\partial z} \quad (7)$$

Surfaces  $S_r$  and  $S_l$  in Fig.1c have different normal directions. Substitute  $z = z_r$  and  $z = z_l$  into Eqs. (6) and (7), then one can get the relation of  $p$  and  $q$  between one node on  $S_r$  and another node on  $S_l$ . Since  $p$  can be expressed as the mean value because the pressure is constant at each pipe end,  $q$  at any node  $i$  on  $S_r$  and  $S_l$  becomes

$$\begin{bmatrix} q_{ri} \\ q_{li} \end{bmatrix} = \begin{bmatrix} t_{11} & t_{12} \\ t_{21} & t_{22} \end{bmatrix} \begin{bmatrix} \frac{1}{n_r} \sum_{j=1}^{j=n_r} p_{rj} \\ \frac{1}{n_l} \sum_{j=1}^{j=n_l} p_{lj} \end{bmatrix} \quad (8)$$

Here  $n_r$  and  $n_l$  are node numbers at each end. Thus, the relation between  $p$  vector  $\mathbf{P}_e$  and  $q$  vector  $\mathbf{Q}_e$  at the two ends can be written as

$$\mathbf{Q}_e = \mathbf{S} \mathbf{P}_e \quad (9)$$

### 3.2.3 Solving simultaneous equations

For the whole problem of flanged waveguide in Fig.1a, one has the Eqs. (3), (4) and (9) of each couple of ends, so the overall system can be assembled. After applying the boundary condition in section 2.2 to the flange and tube walls and solving the overall system, the values of  $p$  and  $q$  for each node on the surfaces  $\Gamma$  and  $S_{jun}$  can be obtained.

## 4. Comparison with known solutions

For simple waveguides and flanges, there are analytical solutions and the BEM works. We calculate the pressure at imaginary ends of the waveguide and the total pressure at a point outside the flange and then compare with the method proposed to check its accuracy. The first example is a straight pipe. The seconde one is a T pipe.

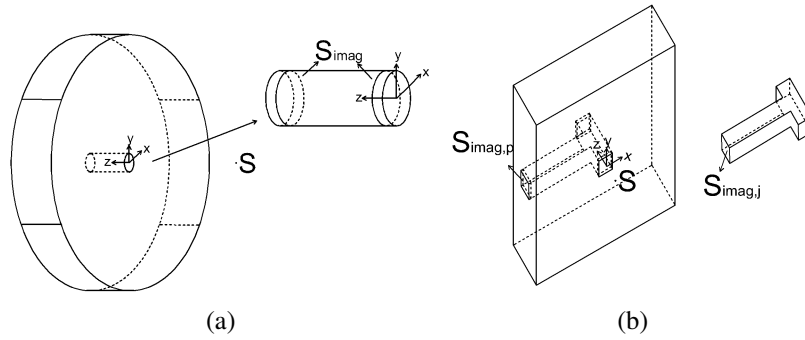


Figure 2: (a) One pipe with cylindrical flange; (b) T pipe with rectangular flange.

### 4.1 Straight pipe

The flange in this example is a cylinder. There is a thin pipe at the center (see Fig.2a). The flange and pipe wall are rigid. The radius of the pipe and the flange is  $0.005m$  and  $0.6m$  respectively. The pipe length is  $0.1m$ . The source  $S$  is at  $(0, 0, -0.1)$ . We create imaginary ends for the pipe to ensure that the pressure is uniform at these ends. The coordinates of the imaginary ends are  $z = 0.005$  and  $z = 0.095$  (see Fig.2a).

#### 4.1.1 Analytical method

The total pressure can be calculated by

$$p_{tot} = p_{rad} + p_{inc} \quad (10)$$

$p_{inc}$  in this part is the incident pressure at point  $R(0.1, 0.1, -0.1)$  from the source and reflected by the flange without waveguide.  $p_{rad}$  is the pressure radiating from the waveguide.

The first step to get  $p_{rad}$  is calculating the pressure  $p_{end}$  and particle velocity  $v_{end}$  at the imaginary ends analytically. Since the pipe is straight and thin, there is only plane wave. One has Eq. (5) and its solution Eqs. (6) and (7). Substitute  $z = 0$  and  $z = l$  into them, one gets the expressions of pressure  $p_{rt}$ ,  $p_{lt}$  and velocity  $v_{rt}$ ,  $v_{lt}$  at the real ends of the pipe. At the two real ends the pressure and velocity include two parts: radiating part and incident part. Substitute them into the expressions of pressure and velocity obtained before. One has

$$p_{rr} \cos kl + i\rho c v_{rr} \sin kl - p_{lr} = -p_{ri} \cos kl - i\rho c v_{ri} \sin kl + p_{li} \quad (11)$$

$$p_{rr} \sin kl - i\rho c v_{rr} \cos kl + i\rho c v_{lr} = -p_{ri} \sin kl + i\rho c v_{ri} \cos kl - i\rho c v_{li} \quad (12)$$

$p_{rr}$  and  $v_{rr}$  are values of wave radiating from the right real end, and  $p_{lr}$  and  $v_{lr}$  are from the left real end.  $p_{ri}$  and  $v_{ri}$  are values of incident wave at the right real end, and  $p_{li}$  and  $v_{li}$  are at the left real end. The pressure and velocity radiating from the pipe satisfy

$$\frac{p_{rr}}{v_{rr}} = -Z_r \quad (13)$$

$$\frac{p_{lr}}{v_{lr}} = Z_r \quad (14)$$

$Z_r$  is the radiation impedance. Since the flange is big compared to the pipe and the source is close to the pipe, the flange can be considered as infinite. One has  $Z_r = \rho c \left( \frac{1}{2}(kr)^2 - i(0.8216kr) \right)$ , where  $r$  is the pipe radius.

From Eqs. (11)-(14) one can obtain a system of linear equations. In this system,  $p_{ri}$ ,  $v_{ri}$ ,  $p_{li}$  and  $v_{li}$  should be given. In Fig.2a if we close the real ends of the pipe and then put rigid boundary condition on the whole surface, these values can be obtained by BEM, and so is the incident pressure  $p_{inc}$  at receiver  $R$  in the exterior domain. After substituting them into the system and solving, one can get the pressures  $p_{rr}$ ,  $p_{lr}$  and velocities  $v_{rr}$ ,  $v_{lr}$  at the two ends for a given frequency.

Then one can get  $a$  and  $b$  from the expressions of pressure and velocity. Substitute them in Eq. (6), one obtains the pressure  $p_{end}$  and  $v_{end}$  at the imaginary ends. With  $p_{end}$ , the pressure  $p_{rad}$  radiating for the pipe can be obtained by BEM. Closing the pipe at imaginary ends in Fig.2a, putting  $p_{end}$  on the end surfaces and rigid boundary condition on the other part of surface, removing the source, and solving this problem by BEM, one has  $p_{rad}$  at  $R$ . Then the total pressure at the point  $R$  can be obtained by Eq. (10).

#### 4.1.2 Comparison

One can solve this problem by the multi-domain BEM (M-BEM) introduced in section 3. There is no junction, so only the Eqs. (3) and (9) are needed.

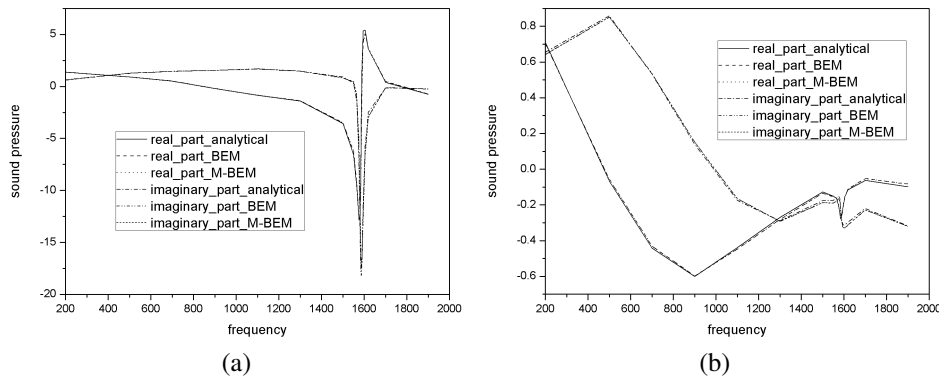


Figure 3: Pressure: (a) At right imaginary end of straight pipe; (b) At point  $R$  near flange

Fig.3a and 3b are the pressures at the right imaginary end of the straight pipe and at point  $R(0.1, 0.1, -0.1)$  calculated by three methods. Good agreement can be seen in these figures. The error of pressure between two different methods can be calculated by  $error = |p_1 - p_2|/|p_1|$ . At point  $R$ , the maximum error between M-BEM and BEM is 2.6%, and the maximum error between M-BEM and analytical method is 7.5%. In the analytical method, the assumption of uniform pressure at the real pipe ends is used. Actually it is not plane wave at the real ends, for the pipe radius changes suddenly. This assumption brings error. Its influence on pressure in the exterior domain is smaller than at the imaginary ends.



## 4.2 T pipe

The flange in this example is a hexahedron. There is a T pipe at the center (see Fig.2b). The flange and pipe wall are rigid. The cross section of the pipe and the flange is  $0.02 \times 0.02m$  and  $0.3 \times 0.3m$  respectively. The pipe length is  $0.1m$  and the branch length is  $0.14m$ . The source  $S$  is at  $(0, 0, -0.1)$ . We create imaginary ends  $S_{imag,p}$  for the T pipe to ensure that the pressure is uniform at these ends. The distance between imaginary ends and real ends is  $0.005m$  (see Fig.2b). Then we create imaginary surfaces  $S_{imag,j}$  for the junction. The distance between  $S_{imag,p}$  and  $S_{imag,j}$  is  $0.005m$ .

In multi-domain BEM, assemble and solve Eqs. (3), (4) and (9) of each couple of imaginary surfaces  $S_{imag,p}$  and  $S_{imag,j}$ , one can get the solution. By Eq. (1) one has the sound pressure field. Fig.4a and Fig. 4b are the pressures at the imaginary end ( $z = 0.005m$ ) and at point  $R(-0.1, 0.1, -0.1)$  calculated by two methods. In Fig.4b there is good agreement. The maximum error of pressure at point  $R$  between M-BEM and BEM is 1.4%.

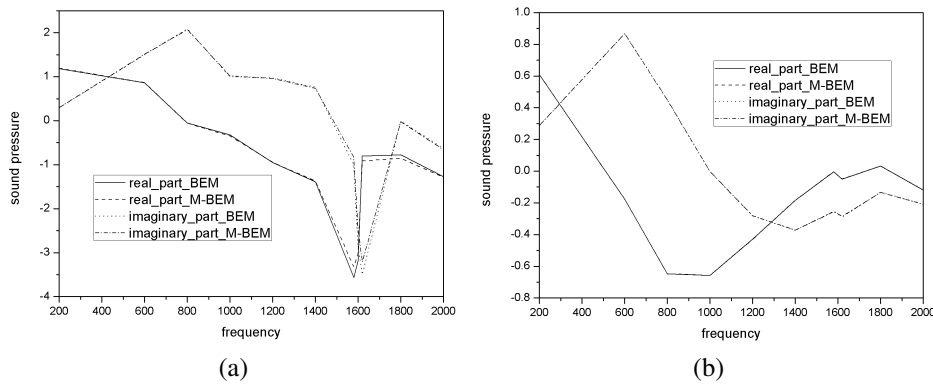


Figure 4: Pressure: (a) At the imaginary end of straight pipe; (b) At point  $R$  near flange

In Fig.4a, one can see good agreement between these two methods except around the resonant frequency which is about  $1600Hz$ . The reason is that the assumption of plane wave in M-BEM is not perfect for this rectangular cross section pipe around  $1600Hz$ .

## 5. Flanged network

A complicated network with four junctions is calculated by multi-domain BEM (see Fig.5a), whereas single domain BEM doesn't work because of too many nodes. Comparison of sound pressure field with rigid flange without network is shown in Fig.5b. The flange size is the same as before. The cross section of pipe is  $a \times a = 0.005 \times 0.005m$ . The flange and network walls are rigid. The source  $S$  is at  $(0, 0, -0.1)$ . The observer  $R$  is at  $(-0.2, 0, 0.05)$ .

Since the cross section of network is small, there is no obvious differences at low frequencies. At high frequencies, one can see big changes of pressure at  $R$ , especially around  $1200Hz$ . Because the pressure of wave radiating from the network is big.

Observer  $R$  is close to straight pipe 1, so around its resonant frequencies there are large differences of pressure. The straight pipe 1 has one open end with flange. The other open end is connected to a complex junction. Its length is  $0.14m$ . To estimate its resonant frequencies, one can simply use the formula for pipe with two open ends. Since the flanges of the open ends are not infinite, one can choose the formula for small flange  $f = c/2l_p$ , where  $l_p = l + 0.6a$ . The resonant frequency is about  $1199.3Hz$  which agrees well with the results in Fig.5b.



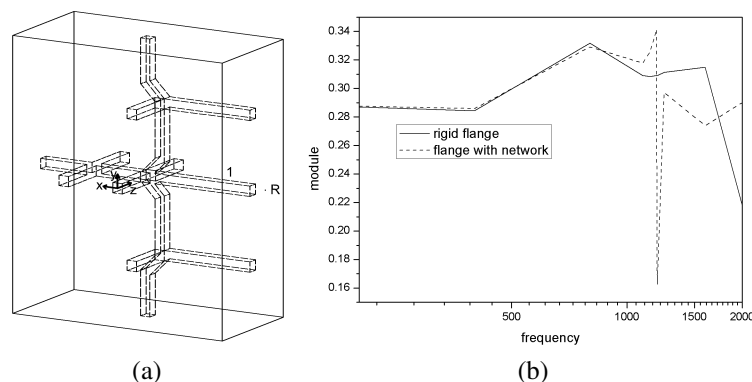


Figure 5: (a) Network with rectangular flange; (b) Module of sound pressure at  $R$

## 6. Conclusion

The multi-domain BEM proposed in this paper makes it possible to calculate the three-dimensional sound pressure field of bodies with macro porosities. It uses substructuring and transfer matrix techniques to reduce nodes, elements and the BEM matrix size and to save computational memory. Only the flange and junctions need to be modeled. It combines the advantages of boundary element method and transfer matrix technique together. The method has good accuracy. It can be applied to the analysis of porous materials and horn effect of tire/road and so on.

## REFERENCES

- <sup>1</sup> Y.-B. Park, H.-D. Ju, S.-B. Lee, Transmission loss estimation of three-dimensional silencers by system graph approach using multi-domain bem, *Journal of Sound and Vibration* 328 (4) (2009) 575–585.
- <sup>2</sup> T.-W. Wu, Multi-domain boundary element method in acoustics, in: *Computational Acoustics of Noise Propagation in Fluids-Finite and Boundary Element Methods*, Springer, 2008, pp. 367–386.
- <sup>3</sup> C. Brebbia, S. Walker, *Boundary Element Techniques in Engineering*, Newnes-Butterworths, 1980.
- <sup>4</sup> C. R. Cheng, *Boundary Element Analysis of Single and Multidomain Problems in Acoustics*, Ph.D. thesis, UNIVERSITY OF KENTUCKY. (1988).
- <sup>5</sup> H. Utsuno, T. W. Wu, A. F. Seybert, T. Tanaka, Prediction of sound fields in cavities with sound absorbing materials, *AIAA Journal* 28 (1990) 1870–1876.
- <sup>6</sup> C. Cheng, A. Seybert, T. Wu, A multidomain boundary element solution for silencer and muffler performance prediction, *Journal of Sound and Vibration* 151 (1) (1991) 119–129.
- <sup>7</sup> M. L. Munjal, M. Munjal, *Acoustics of ducts and mufflers with application to exhaust and ventilation system design*, Wiley New York (NY) et al., 1987.
- <sup>8</sup> A. Craggs, D. Stredulinsky, Analysis of acoustic wave transmission in a piping network, *The Journal of the Acoustical Society of America* 88 (1990) 542.
- <sup>9</sup> G. Lou, T. Wu, C. Cheng, Boundary element analysis of packed silencers with a substructuring technique, *Engineering Analysis with Boundary Elements* 27 (7) (2003) 643–653.
- <sup>10</sup> D. Duhamel, *L'acoustique des problèmes couples fluide-structure-application au contrôle actif du son*, Ph.D. thesis, Ecole des Ponts ParisTech (1994).